Applied Surface Science 442 (2018) 602–612

Contents lists available at ScienceDirect

Applied Surface Science

journal homepage: www.elsevier.com/locate/apsusc

Full Length Article

Surface characterization and free thyroid hormones response of chemically modified poly(ethylene terephthalate) blood collection tubes

Ebrahim Jalali Dil [a], Samuel C. Kim [b], Amir Saffar [a], Abdellah Ajji [a], Richard N. Zare [c], Annie Sattayapiwat [c], Vanessa Esguerra [c], Raffick A.R. Bowen [c,*]

[a] Ecole Polytechnique de Montreal, Montreal, QC, Canada
[b] University of California, San Francisco, San Francisco, CA, USA
[c] Stanford University, Stanford, CA, USA

ARTICLE INFO

Article history:
Received 7 December 2017
Revised 9 February 2018
Accepted 17 February 2018
Available online 22 February 2018

Keywords:
Blood collection tube
Polyethylene terephthalate
Surface modification
Free triiodothyronine
Free thyroxine
Thromboelastography

ABSTRACT

The surface chemistry and surface energy of chemically modified polyethylene terephthalate (PET) blood collection tubes (BCTs) were studied and the results showed a significant increase in hydrophilicity and polarity of modified PET surface. The surface modification created nanometer-sized, needle-like asperities through molecular segregation at the surface. The surface dynamics of the modified PET was examined by tracking its surface properties over a 280-day period. The results showed surface rearrangement toward a surface with lower surface energy and fewer nanometer-sized asperities. Thromboelastography (TEG) was used to evaluate and compare the thrombogenicity of the inner walls of various types of BCTs. The TEG tracings and data from various types of BCTs demonstrated differences in the reactionand coagulation times but not in clot strength. The performance of the modified tubes in free triiodothyronine (FT_3) and free thyroxine (FT_4) hormone tests was examined, and it was found that the interference of modified PET tubes was negligible compared to that of commercially available PET BCTs.

1. Introduction

The use of plastic materials to manufacture blood collection tubes (BCTs) has received much attention due to the ease of processing, handling, and disposing of plastic and the lower production cost of plastic BCTs compared to glass BCTs. Among various polymers, poly(ethylene terephthalate), PET, has commonly been used due to its transparency and light weight. However, PET-based BCTs can have complex interactions with blood that may alter the composition of the blood or its serum and plasma fractions and in some cases may adversely affect laboratory tests that are performed on blood specimens As a consequence of the multiple, complex interactions of collection devices with blood specimens, collection devices can be a major source of potential error in the pre-analytical phase of laboratory testing [1]. Manufacturers have recognized this problem and have tried to overcome this interference by coating the walls of the PET BCTs with surfactants. However, previous studies have indicated that this approach can pose a new problem in that the surfactants can leach out of the walls and interfere with various tests [2]. To avoid surfactant use and its consequences, the PET surface has been modified to make it hydrophilic. The literature shows that PET surface modification has been achieved using various methods, including modification by UV irradiation and plasma etching, both of which have received much attention [3–10]. Previous studies on plasma-treated PET have shown a loss of surface hydrophilicity over storage time, which can significantly affect the performance of BCTs [11–13]. A previous study from this group introduced a simple chemical procedure in which ethylene glycol is grafted to PET BCT surface and caused the surface to become hydrophilic, closely resembling the behavior of glass BCTs; such tubes are called "chemoPET" [14]. It should be noted that poly(ethylene glycol), PEG, is often used to modify plastic surfaces because PEG polymer is known to passivate hydrophobic surfaces and render them more bio-compatible (e.g., improved cell viability, reduced nonspecific adsorption of biomolecules). Grafting of PEG, also known as PEGylation, is commonly performed via crosslinking chemistry between functionalized PEG chains and a plastic surface. In contrast, the reported surface modification method in our previous study [14] is based on glycolysis of PET. In this method, the tetramethylguanidine (TMG), which is a strong base, serves as a catalyst for trans-esterification reaction. The ester bond connecting monomeric units of PET is broken

* Corresponding author at: Stanford Health Care, 300 Pasteur Drive, Room H-1401J, Stanford, CA 94305, USA.
E-mail address: rbowen@stanfordhealthcare.org (R.A.R. Bowen).

https://doi.org/10.1016/j.apsusc.2018.02.177
0169-4332/

and a new ester bond is formed between ethylene glycol (EG) and terephthalic acid. The end product is the PET surface decorated with covalently conjugated EG molecules. The strong basicity of TMG makes this reaction very efficient such that incubation at room temperature is enough for complete surface modification. It is also noteworthy that both EG and TMG are much less expensive than PEG polymer and crosslinker used in common surface modifications. Despite these interesting results, detailed surface characterization of the modified PET is necessary to determine the effect of modifying on the surface chemistry, surface composition, surface energy, and surface topography. In addition, evaluating the applicability of a modification method requires examining the stability of the modified surface and evaluating the performance of the BCTs after long storage times. Therefore, a detailed characterization of the modified PET surface must be conducted using advanced surface-characterization techniques that can determine the surface chemistry and surface energy. Furthermore, in order to study the effect of storage time, surface dynamics and molecular rearrangements in the modified PET must be examined by tracking the surface energy, topography, and surface chemistry of the modified PET over long storage times. The molecular mechanisms involved in the observed changes in topography and surface energy are discussed herein. Thromboelastography (TEG) has been used to characterize the coagulant state of blood or plasma specimens in vitro [15]. In TEG analysis, the viscoelastic changes that occur during coagulation are monitored and analyzed, and the results are presented in the form of TEG tracings, which provide data on the initiation of clotting, the formation of the clot, and its stability [15]. TEG has been used to characterize the coagulant nature of biomaterials with blood components, including platelets and blood cells [16]. Recently, TEG was used to evaluate commercially available Greiner Bio-One blood clotting activator (BCA™) tubes and Becton Dickinson (BD) lithium heparin and BD rapid serum tubes (RST™) serum separator tubes [17]. Therefore, it will be interesting to compare thrombogenicity of the surfaces of the chemoPET tube wall interiors to that of commercially available plastic and glass BCTs. Finally, the performance of chemoPET BCTs in free triiodothyronine (FT_3) and free thyroxine (FT_4) hormone tests was examined after the storage period.

2. Experimental

2.1. Materials

PET (Laser+ 7000) granules with a bulk density of 0.833 g/cm^3 were purchased from DAK Americas. Ethylene glycol (EG) and 1,1,3,3 tetramethylguanidine (TMG) were purchased from Sigma-Aldrich (St. Louis, MO). Glycerol (GL) (>99.5% pure) was obtained from Invitrogen (Carlsbad, CA). This study examined six types of blood collection tubes: (1) a plastic Vacuette™ (gold-top tube with gel separator; 13 × 75 mm, cat. no. 454228; lot B041406, Monroe, NC); (2) a glass tube (a red-top Vacutainer™ no-additive blood tube; 16 × 100 mm, cat. no. 366441; lot 4034472); (3) a plastic SST™ tube (a gold-top Vacutainer™ tube with gel separator; 13 × 75 mm, cat. no. 367983; lot 4030600); (4) a plastic rapid serum tube (RST™) (orange-top Vacutainer™ tube with gel separator; 13 × 100 mm, cat. No. 368774; lot 140708); (5) a plastic plain red-top (PRT) tube (a Vacutainer™ tube with no gel separator; 13 × 100 mm, cat. no. 367814; lot 4079576); and (6) chemically modified tubes made from unmodified PET tubes (BD, 3-mL Vacutainer™ discard tubes with no interior coating; cat. no. 366703; lot 2160209).

2.2. Film sample preparation

PET granules were dried at 100 °C overnight in a vacuum oven before processing. PET film with a thickness of 25 μm was prepared using a twin-screw extruder (LEISTRITZ Extruder; Germany) with an 18-mm screw and L/D = 40. The cast film extrusion was carried out at a temperature profile of 250–270 °C and at 150 rpm. The film was collected immediately after the cast rolls and stored in a sealed polyethylene bag to avoid surface contamination.

2.3. Surface modification

The chemically modified PET film and the tubes used in this study were prepared following the protocol outlined in a previous study [14]. Fig. 1 shows a schematic of the modification reaction. Briefly, 5 mL of 40% (v/v) TMG solution in EG was poured into unmodified (discard) PET tubes and incubated at room temperature (22 °C) for 30 min. After incubation, the TMG/EG solution was collected for the next batches of reactions, and the plastic tubes were rinsed with deionized water and dried at room temperature overnight while protected from dust. The same procedure was followed for PET film samples. As previously described, the modified chemoPET tubes contained no detectable contaminants (e.g., volatiles) from the chemical reaction [14]. Throughout this paper, the unmodified and surface-modified PET films will be called PET and chemoPET, respectively. After surface modifications, the samples were sealed in plastic bags to avoid surface contamination during handling and storage.

2.4. X-ray photoelectron spectroscopy

X-ray photoelectron spectroscopy (XPS) measurements were conducted using a VG ESCALAB 3 MKII spectrometer (VG) (Thermo Electron Corporation, UK) with an Mg Kα ray source. The measurements were performed at 90° and 20° electron take-off angles, which resulted in analysis depths of 10 nm and 3.9 nm, respectively. The relative atomic percent was calculated from the relative peak areas, which were corrected by the Wagner sensitivity factors and the Shirley background subtraction.

2.5. Time-of-flight secondary ion mass spectrometry

The film samples were mounted on the sample holder using double-sided tape. Time-of-flight secondary ion mass spectrometry (ToF-SIMS) measurements were done using an ION-TOF SIMS IV apparatus (Munster, Germany) with an operating pressure of 5×10^{-9} Torr (6.7×10^{-7} Pa). First, the sample was bombarded with Bi_3^+ at an energy of 15 keV in bunch mode. The gun was operated with a 100-ns pulse width and a 0.3-pA pulsed ion current to produce a dosage that was higher than 5×10^{11} ions cm^{-2} but below the threshold level of 10^{13} ions cm^{-2} for static SIMS. Charge neutralization was achieved with an electron flood gun. Secondary ion spectra were obtained from an area that measured 50 × 50

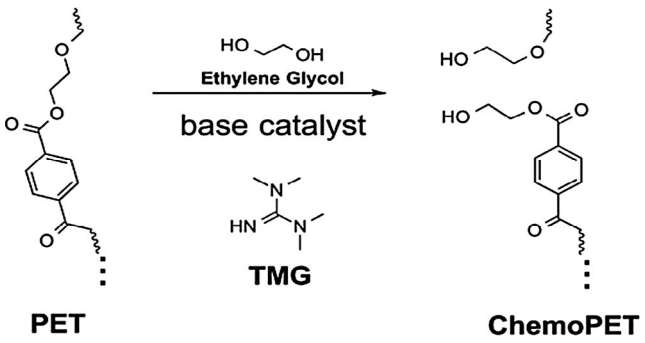

Fig. 1. Schematic of the PET surface modification reaction.

μm^2 using 128 × 128 pixels (1 pulse per pixel) and at least 4 different positions per sample.

2.6. Sessile drop measurements

Sessile drop measurements were carried out using an automated sessile drop machine (OCA20; Dataphysics; Germany). Droplets of 2 μL were injected using a syringe with a diameter of 0.52 mm and were placed on the surface of the film samples. The surface energy of the samples was determined by measuring the contact angles of water, EG, and formamide as liquid probes. Then, the Owens-Wendt [18] approach was used to determine the surface energy and its dispersive and polar components. The surface energy data for the liquid probes were taken from the literature [19].

2.7. Atomic force microscopy

The surface topography of the film samples was examined using an atomic force microscopy (AFM) machine (NanoScope V Dimension Icon/Fastscan AFM; Bruker; USA) operated in tapping mode in air. All imaging was acquired using intermittent peak force tapping™ using 125-μm TESPA Air probes. The roughness measurements were taken on an area of 50 × 50 μm^2. The roughness of the samples was determined by image analysis using NanoScope Analysis software (V 1.5; Bruker). The roughness values reported are the averages of five different measurements.

2.8. Thromboelastography

The type of blood collection tubes used, transport, and processing of blood specimens from apparently healthy volunteers were all as previously described [1]. To evaluate the interior surface of the BCTs using TEG, a procedure as described by Dimeski et al. [17] was followed. Briefly, 4.5-mL sodium citrate tubes (3.2%) were used to collect whole blood specimens from apparently healthy volunteers. Then, 1-mL aliquots of whole blood from the citrate tube from each volunteer were placed into each of the four different types of tube. The blood was recalcified using 200 mM of $CaCl_2$, and the tubes were capped and inverted 10 times to ensure that the whole blood was in contact with the tube's entire wall surface. After mixing, a 340-uL aliquot from each tube was added to a TEG cup, and TEG analysis was initiated. The three TEG parameters of interest were: (1) the reaction time (R), which is the time it takes the curves to diverge with an amplitude of 2 mm, as the initial clot formation is detected; (2) the coagulation time (K), which is the period from the start of clot formation to when the curves diverge with an amplitude of 20 mm; and (3) the maximum strength of the developed clot (MA), which is the maximum amplitude between the two curves (millimeters; mm) [17].

2.9. Determination of FT_3 and FT_4 concentrations

Serum FT_3 and FT_4 concentrations from apparently healthy volunteers collected in six different types of blood collection tube were measured in a random order on an Immulite™ 1000 analyzer, according to the manufacturer's instructions [13]. During the study, 1 reagent (FT_3 lot: 0402; FT_4 lot: 0362) and 1 calibrator (FT_3 lot: LF3L 0142; FT_4 lot: LFT4L 01388) were used for the Immulite™ 1000 analyzer. Quality-control samples for each of these assays will also be tested and evaluated for satisfactory performance before serum samples from the various tube types were tested.

2.10. Statistical analysis

The sample size calculation with an 80% power to detect a clinically significant difference in thyroid hormone levels among tube types has been described previously [14]. For the FT_3 and FT_4 concentrations in the various BCTs, singleton measurements were used for statistical analysis, and the results were reported as the mean ± (SD). The Wilcoxon-Mann-Whitney test was used to test for statistical difference between free thyroid hormone concentrations measured from the various BCTs and compared to those measured from glass tubes. The Bonferroni method was used to conservatively adjust the significance level to $p < 0.00833$ (=0.05/6 tube types). Statistical analyses were performed using Analyze-It™ for Microsoft Excel (version 1.71; Analyze-It Software; Leeds, UK). The clinical relevance of the statistically significant differences in analyte concentrations among the tube types was determined using the significant change limit method, as described previously [14].

3. Results and discussions

3.1. Surface chemistry analysis

Due to the difficulties in the surface characterization of PET tubes, which arises mainly from the curvature of their inner surface, PET and ChemoPET films were used as model systems in the surface characterizations. It should be mentioned that the same modification procedure was followed exactly for both film and tube samples. The surface chemistry of PET and chemoPET was evaluated using XPS analysis, and Fig. 2 presents the results. In addition, Table 1 lists a summary of the XPS survey spectra. The XPS results recorded at the electron take-off angle of 90° show a carbon-to-oxygen ratio (C/O) of 2.4 for the PET sample. This value is very close to the theoretical C/O ratio of 2.5 in a PET molecule and confirms the PET nature of the surface. The C/O ratio of the chemoPET at this electron take-off angle was determined as 2.2, which indicated a higher concentration of oxygen at the surface of the chemoPET compared to the PET.

In order to increase the contribution of the uppermost layers in the XPS results, the electron take-off angle was reduced to 20°, which reduced the analysis depth to 3.9 nm. Reducing the take-off angle from 90° to 20° increased the gap between the C/O ratios of the PET and the chemoPET, which confirmed a much higher oxygen concentration on the surface of the chemoPET sample.

Considering the reaction scheme shown in Fig. 1, the modification reaction increases the ratio of C—O/C=O in the modified mole-

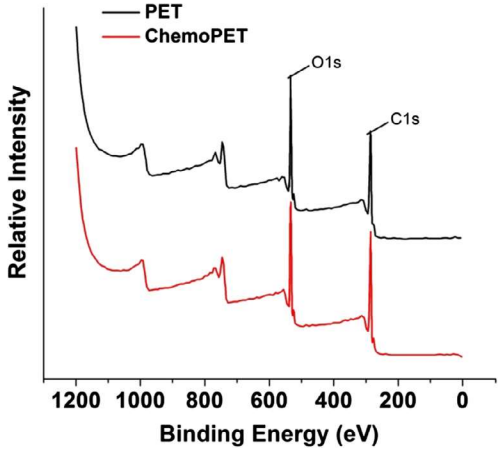

Fig. 2. XPS survey spectra of the PET and chemoPET samples.

Table 1
XPS analysis results of non-modified and modified PET film samples obtained from XPS survey scans.

Name	Binding Energy (eV)	Atomic %			
		Electron take-off angle = 90°		Electron take-off angle = 20°	
		PET	ChemoPET	PET	ChemoPET
C1s	285.0	70.6	69.0	74.3	67.8
O1s	532.3	29.4	31.0	25.7	32.2
C1s/O1s	–	2.4	2.2	2.9	2.1

cules compared to the ratio in the neat PET. The ratio of C—O/C=O was examined using high-resolution XPS performed at the 20° electron take-off angle (=3.9 nm analysis depth) in the oxygen (O1s) and carbon (C1s) regions and the results are shown in Fig. 3.

High resolution results indicated that the ratio of C—O/C=O increased from 0.94 to 1.02 in O1S spectrum and from 1.03 to 1.11 in C1s spectrum. These results confirmed the presence of a higher oxygen and C—O bond concentration, which can be attributed to the presence of the reacted EG groups at the surface of the chemoPET.

ToF-SIMS analysis was used in order to confirm the presence of reacted EG molecules in the uppermost layers of the chemoPET sample. Considering its very thin analysis depth (=10 Å), this technique allows a much deeper understanding of the compositions of the surface layers.

Fig. 4 shows the obtained ToF-SIMS spectra for the PET and chemoPET samples. The presence of characteristic peaks at m/z = 357, 313, 209, 191, 165, 121, and 76 in the negative ions spectra and peaks at m/z = 385, 341, 237, 193, 149, 121, and 104 in the positive ions spectra confirmed the PET nature of the examined surfaces [20,21].

Li et al. [22] proposed a semi-quantitative method to compare the chemical composition at the surface of two samples using ToF-SIMS analysis. In this method, characteristic peaks are treated using the following equation:

$$I_n = \frac{I_i^1 / I_t^1}{I_i^2 / I_t^2} \quad (1)$$

where I_i^1 and I_t^1 are the intensity of peak at m/z = i in sample 1 and the total intensity of the mass range for sample 1. I_i^2 and I_t^2 are the same as I_i^1 and I_t^1, but for sample 2.

As Fig. 5 shows, the values of I_n for characteristic peaks are close to 1, except for m/z = 237 and 209 in the positive and negative spectra, respectively. As shown in Fig. 5, these peaks correspond to the fragments, with EG end groups attached to the carboxyl group. These results along with the XPS results clearly confirm the higher concentration of EG groups on the uppermost layers of the surface of the chemoPET.

Fig. 6 shows a typical O^- and OH^- ions distribution in the 2D ToF-SIMS ion mapping of the PET and chemoPET samples. By considering the PET sample as the control sample, a uniform distribu-

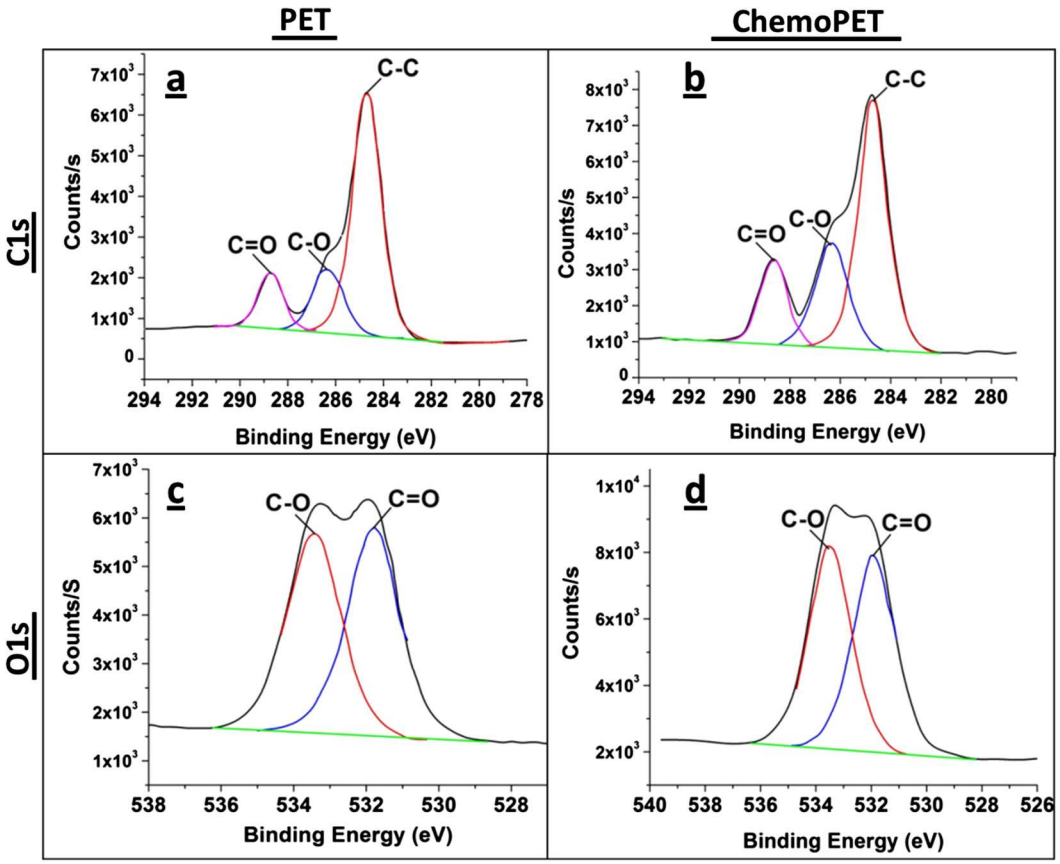

Fig. 3. XPS high-resolution spectra of the surface of PET and ChemoPET in the carbon (C1s) and oxygen region (O1s).

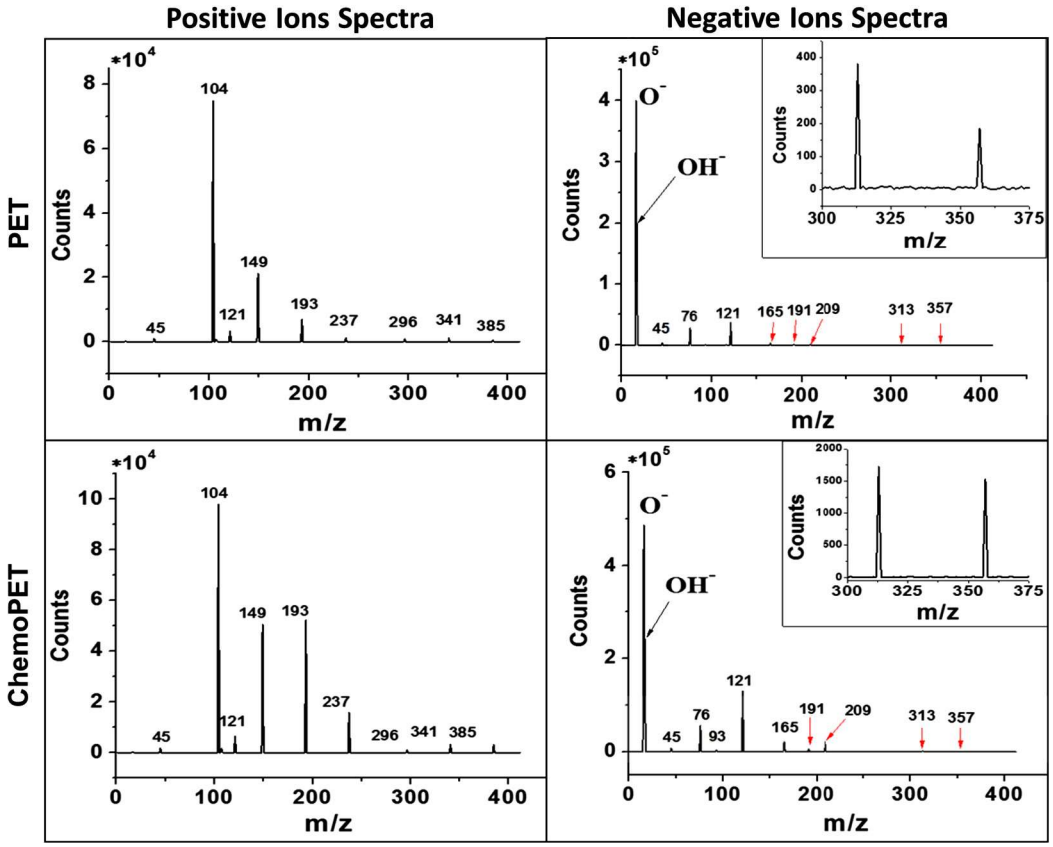

Fig. 4. ToF-SIMS spectra of the PET and chemoPET samples. The inserts in the negative ions spectra show higher magnification of negative ion masses above m/z = 300 amu.

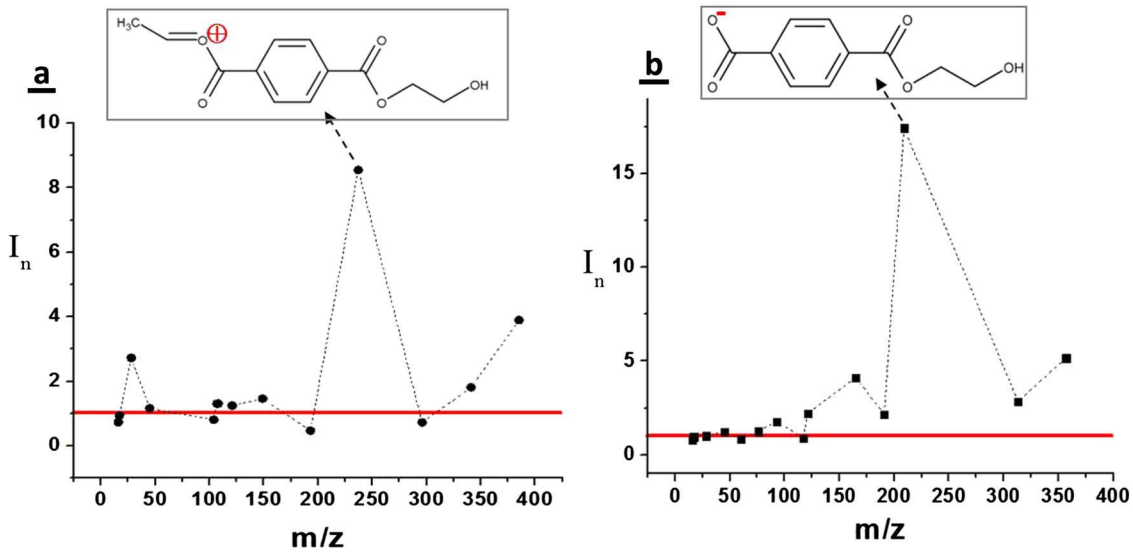

Fig. 5. Comparison the intensities of ToF-SMS characteristic peaks in (a) the positive ions spectra and (b) the negative ions spectra. The red straight lines show I_n = 1. (For interpretation of the references to color in this figure legend, the reader is referred to the web version of this article.)

tion of ions emitted from the surface indicated a uniform distribution of oxygen and a uniform modification of the chemoPET surface.

3.2. Surface energy analysis

To determine the effect of surface modification on the hydrophilicity and surface tension of the PET film, the surface tension of the PET and chemoPET were evaluated using the sessile drop test. Fig. 7 shows the drop images of various liquid probes on the surfaces of the PET and chemoPET films. Table 2 lists the calculated surface tensions and the surface-tension components of these samples.

As can be seen, the surface modification increases both the surface's tension and its polarity. It should be noted that the polar component of the surface energy represents the ability of the

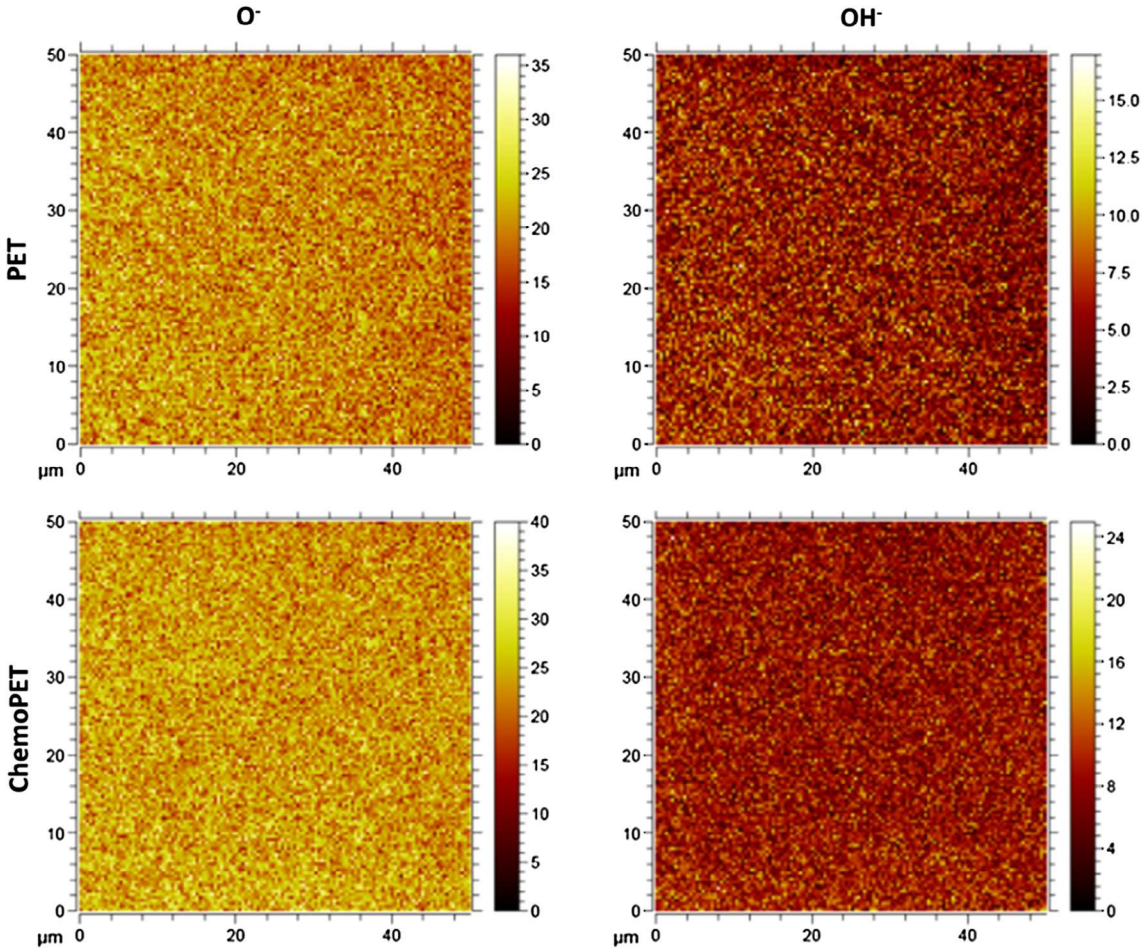

Fig. 6. The 2D ToF-SIMS ion mapping of O^- and OH^- ions in the PET and chemoPET samples.

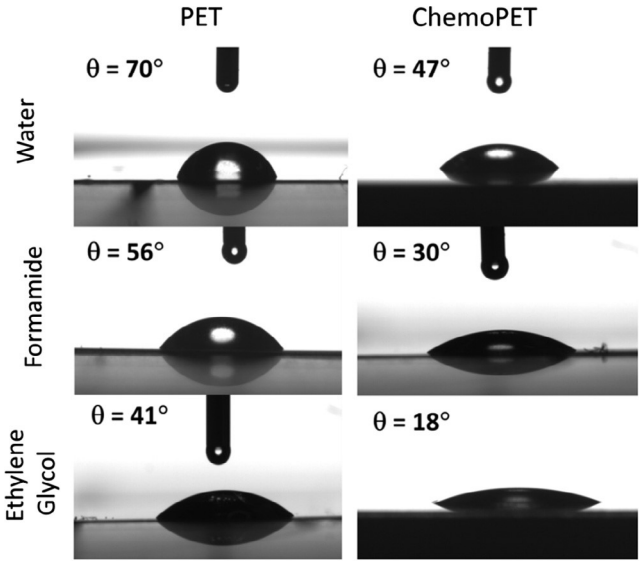

Fig. 7. The effect of surface modification on the contact angle of the liquid probes on the surface of the PET and chemoPET films.

surface to form hydrogen-bonding and polar/polar interactions, indicating a very hydrophilic surface [23]. The surface-tension results were in line with the XPS and ToF-SIMS results and showed an increase in the hydrophilicity and polar-group concentration at the surface of the chemoPET sample compared to the PET one. The surface tension of the PET and chemoPET were also estimated using the empirical equation, presented by van Krevelen [24]:

$$\gamma \approx 0.75(\mathrm{C.E.D})^{2/3} \tag{2}$$

In this equation, C.E.D is the cohesive energy density and can be estimated using the following equation, presented by Bicerano [25]:

$$\frac{E_{co}}{v} = \frac{10570.9({}^{0}\chi^{v} - {}^{0}\chi) + 9072.8({}^{2}\chi - {}^{1}\chi^{v}) + 1018.2N_{VKH}}{v} \tag{3}$$

Here, E_{co}, v, and N_{VKH} are cohesive energy, the molar volume of the repeat unit, and the van Krevelen dimensionless number. In addition, ${}^{0}\chi$, ${}^{0}\chi^{v}$, ${}^{1}\chi$, and ${}^{1}\chi^{v}$ are the zeroth- and first-order connectivity indices, which can be estimated using the procedure presented by Agrawal et al. [26]. Using this approach, the surface tensions of the PET and chemoPET were estimated as 41.25 mN/m and 60.84 mN/m, respectively. A good agreement between the estimated surface tensions and the experimentally measured ones indicated the reliability of this estimation method. The greater difference between the estimated surface tensions and the experimental results for chemoPET can be attributed to the presence of both modified and unmodified PET repeat units at the surface of the chemoPET. It has been shown that the surface tension of a sample composed of two randomly distributed repeat units can be estimated using the linear mixing rule and the surface tensions of each repeat unit [23]. Using the estimated surface energy of the PET and

Table 2
Surface tensions and surface-tension components of PET and chemoPET.

Sample	γ (mJ/m^2)	γ^p (mJ/m^2)	γ^d (mJ/m^2)	Polarity (γ^p/γ)
PET	37.6	10.7	26.9	0.28
ChemoPET	53.4	41.8	11.6	0.78

γ: Surface tension; γ^p: polar component of the surface tension; γ^d: dispersive component of the surface tension.

chemoPET and the experimentally measured surface tension of the chemoPET, the composition of the modified repeat units at the surface of the chemoPET was estimated to be a mole fraction of 62%.

3.3. Surface topography

In addition to the surface chemistry and surface tension, the surface topography is an important characteristic of a surface that can affect some macroscopic properties [27]. AFM imaging was used to investigate the effect of surface modification on the surface topography and the results are shown in Fig. 8. Comparing surface topography of the PET and chemoPET samples show a clear shift toward a surface with needle-like asperities in the AFM images of the chemoPET sample. Image analysis indicated a drop in the root mean square roughness (R_q) of the PET from 49.0 ± 2.2 nm to 16.8 ± 2.8 nm, which indicates a much smoother surface of the chemoPET sample. A shift in the surface topography caused by creating nanometer-scaled features has been reported in PET modified by plasma [5,6,28] and UV [29–32] and has been attributed to the effect of irradiation and/or the agglomeration of grafted molecules [28,33,34]

Due to the small molecular weight of EG, phase separation of the grafted EG molecules cannot be responsible for the needle-like asperities observed in the chemoPET. Estimating the Hansen solubility parameters using the group contribution method [24,26] indicated values of 20.9 MPa$^{1/2}$ and 31.8 MPa$^{1/2}$ for the PET and chemoPET molecules, respectively. It should be noted that the estimated Hansen solubility parameter for PET was very close to the experimental value of 20.5 MPa$^{1/2}$ reported for the PET [35], indicating the reliability of this approach for estimating solubility parameters. The very different solubility parameters for the PET and chemoPET molecules indicates a high potential for molecular segregation and phase separation between the modified and unmodified PET molecules at the surface. Therefore, the needle-like features observed can be attributed to the molecular segregation between the modified and unmodified PET molecules at the surface of the chemoPET sample.

3.4. Surface dynamics of ChemoPET

One of the important aspects of surface-modified materials is the stability of surface modification over time. It is known that polymer molecules at the surface rearrange themselves to reduce the system's surface energy [22]. In the present study, because the modification reaction increased both surface tension and surface polarity, it should have triggered surface rearrangement that reduces the surface energy. Previous studies of surface-modified PET have reported changes in surface tension and surface properties over time, and surface rearrangement has been confirmed in surface-modified PET samples [5,7]. However, considering the very slow diffusion rate of polymer chains, even in the molten state [36], most previous works have studied the surface properties of

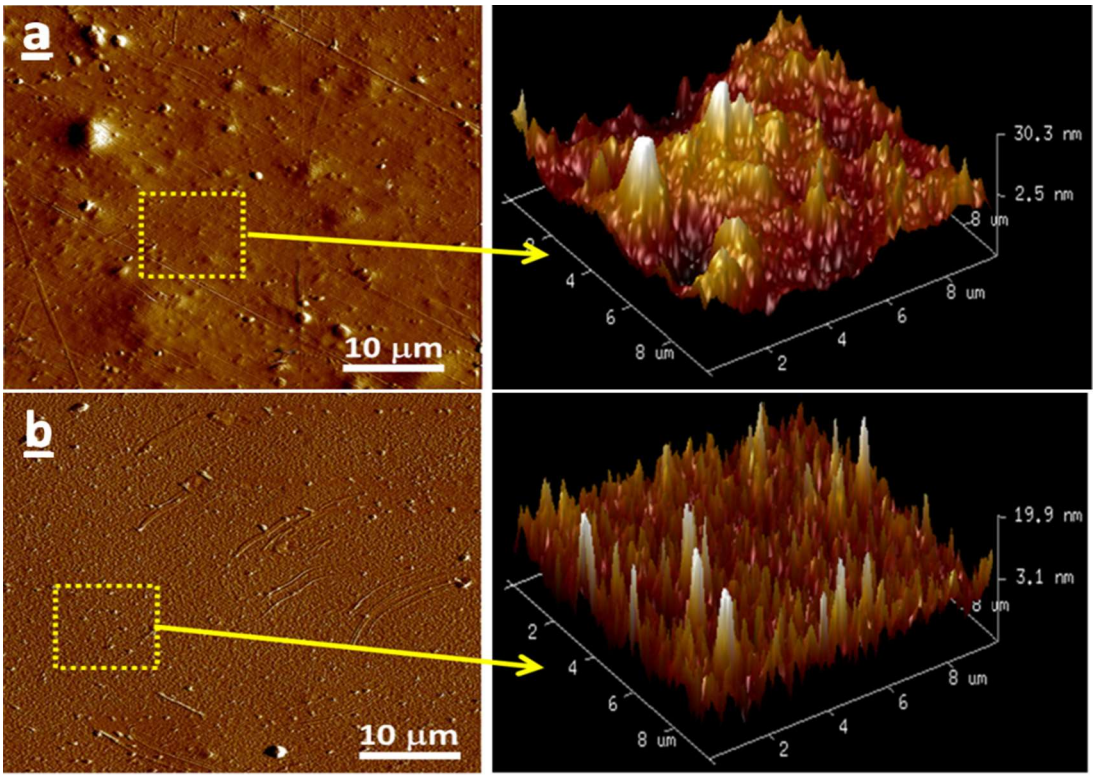

Fig. 8. AFM images of the surface topography of (a) PET and (b) chemoPET. The images on the right show higher magnifications of the surface topography in the marked area.

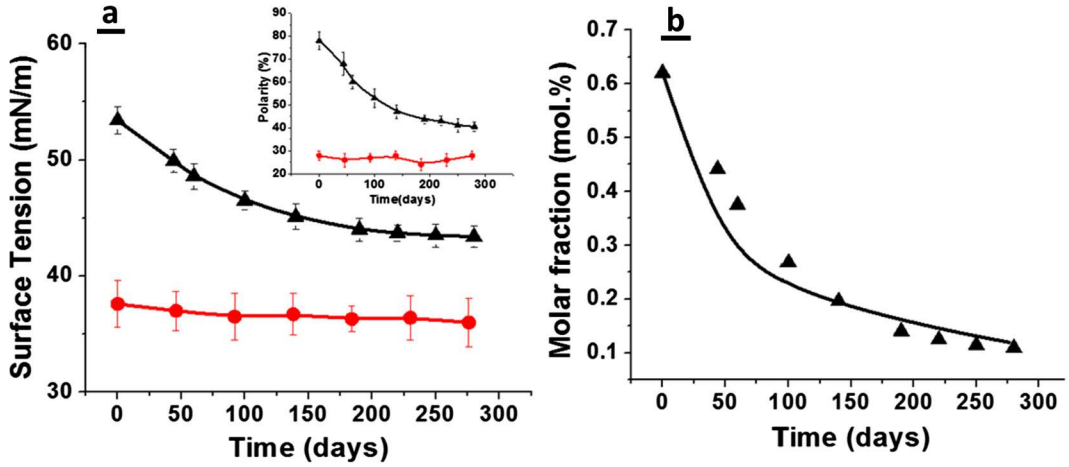

Fig. 9. (a) The PET (circle) and chemoPET (triangle) surface tension over time. The insert graph shows the polarity of the PET and chemoPET samples at various times; (b) the estimated concentration of modified molecules at the surface of the chemoPET. The solid line in (b) shows the fitted diffusion model with d = 7.3×10^{-23} cm^2/s. The error bars in (a) represent standard deviations.

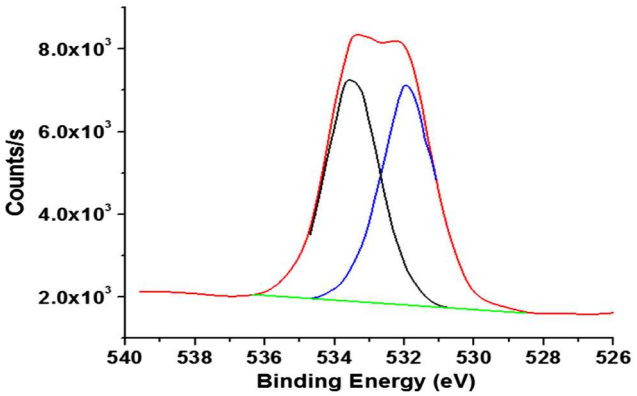

Fig. 10. High-resolution XPS scan of the chemoPET surface after 280 days.

modified polymers over a short period. The present study evaluated the surface dynamics of the modified samples by tracking the surface tension of the PET and chemoPET samples over 280 days, and the results are shown in Fig. 9. It is worth noting that, to our knowledge, this is the longest period that the surface energy of polymeric materials has been tracked to date.

It can be seen that both the surface energy and polarity of the PET sample remain unchanged within the limits of experimental error. In contrast, the surface tension and polarity of the chemoPET sample decreased, approaching a plateau after 190 days. However, even after 280 days, the chemoPET's surface energy and polarity were greater than those of the PET sample. For instance, after 280 days, the polarity of the chemoPET sample was still 44% higher than that of the PET sample. These results indicate the stability of the hydrophilic nature of the chemoPET's surface after long storage. As mentioned previously, the chemoPET's surface composition could be estimated using the linear mixing rule and the estimated surface energies of the modified and unmodified repeat units. The present study used this approach to estimate the mole fraction of the modified PET molecules at the surface, and the results are shown in Fig. 9(b). Over 280 days, aging reduced the composition of the modified PET molecules at the surface from 62 mol% to 11 mol%. The diffusion coefficient for modified polymer chains can be estimated using their molar fraction over time and by assuming a Fickian diffusion regime at the uppermost layers of the surface. The present study used this approach to estimate a diffusion coefficient of 7.3×10^{-23} cm^2/s for the inward diffusion of the modified PET molecules at the surface.

To examine the surface composition of the aged sample, a high-resolution XPS spectrum of the chemoPET was taken after 280 days, and the results are shown in Fig. 10. Aging reduced the ratio

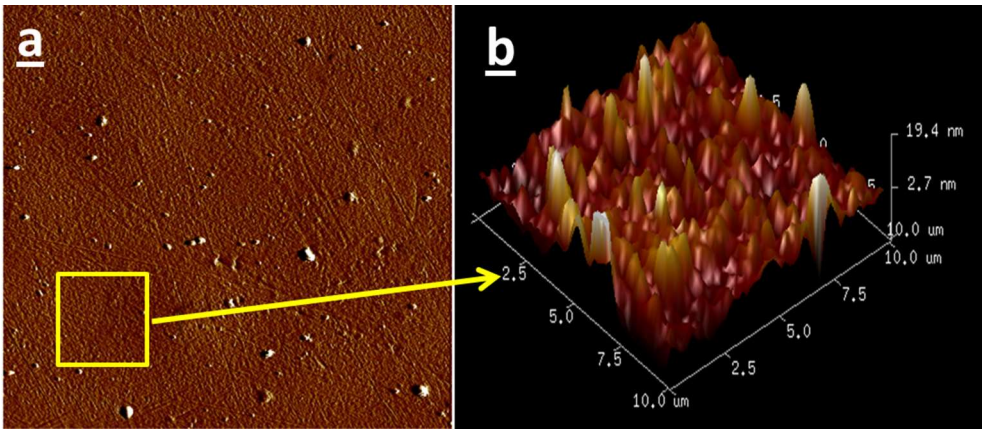

Fig. 11. The effect of storage time (280 days) on the roughness of the surfaces.

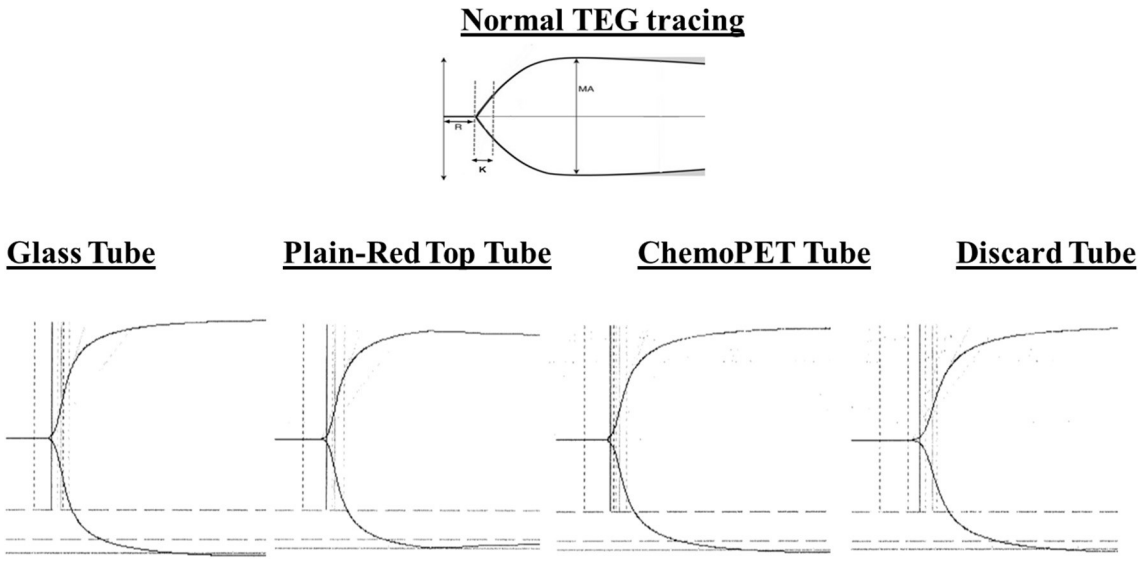

Fig. 12. TEG tracings from various BCT types.

Table 3
The TEG parameters of various BCTs.

	Unit	Glass Tube	PRT Tube	ChemoPET Tube	Discard Tube
R (Reaction Time)	min	8.0	9.0	9.3	12.1
K (Coagulation Time)	min	1.6	1.4	1.7	2.2
MA (Maximum Amplitude)	mm	79.7	75.9	76.5	75.3

of C—O/C═O from 1.02 to 0.97, which indicated a lower concentration of modified molecules at the surface. All the results mentioned above indicated surface rearrangement of the chemoPET over time, resulting in reduced surface energy by reducing the composition of the reacted molecules at the surface.

Considering the previous results confirming surface rearrangement, it was of interest to identify the effect of time on the surface topography of the chemoPET sample. Fig. 11 shows AFM images of the surface of the chemoPET films after 280 days of aging.

Image analysis indicated that the Rq of the chemoPET increased to 29 ± 7 nm after 280 days of aging. Comparing this image with the surface topography of the chemoPET immediately after modification (Fig. 8(b)) showed that aging eliminated the smaller needle-like asperities in the chemoPET and increased its roughness. This result was in agreement with those in other discussions of surface rearrangement and can be attributed to the tendency to reduce the chemoPET's surface energy by reducing its surface area with air. For comparison, the R_q of the PET sample was also examined after 280 days, and aging had reduced its roughness slightly, to 44 ± 5.1 nm.

All the results above indicated that the surface chemistry and topography of the chemoPET changed over time, reducing the system's total surface energy.

3.5. TEG evaluation of interior wall surfaces of tubes

Fig. 12 and Table 3 show the TEG tracings and data, respectively, from the surfaces of the tube wall interiors. The TEG tracings and data showed that when the plastic PRT and the chemoPET tube were compared to a glass tube, the R, K, and MA values were comparable. In contrast, when the plastic discard tube was compared to the glass tube, the R and K times were significantly longer (Fig. 12 and Table 3). The MA of the discard tube was similar to that of the glass tube. Together, these data indicated that blood collected in a discard tube takes longer to initiate and form clots than blood collected in a plastic PRT or a chemoPET tube; however, once formed, the clot has the same MA as the blood collected in the other tube types.

Glass tubes are made of borosilicate and can activate the clotting cascade via the intrinsic (contact) pathway when the factor XII in blood contacts the hydrophilic interior wall surface of glass tubes [37]. The clotting process in glass tubes is fast and produces a solid clot without using clot activators. These findings explain the relatively short Rs and Ks and the strong clotting observed with glass tubes. The longer Rs and Ks for discard tubes compared to glass tubes can be explained by the hydrophobicity of the surfaces of the interior walls of the discard tubes, which is known to prolong Ks [37]. This explains the rational for using both plastic blood collection tubes that contain clot activators, including silica, kaolin, bentonite, and diatomaceous earth and thrombin, to promote rapid clotting through the intrinsic (contact) pathway and for using tubes with thrombin, ellagic acid, and thromboplastin to activate clotting via the extrinsic pathway [1]. Surfactants may also be added to help distribute the clot activators over the surface of the tube wall and reduce the adherence of platelets, fibrin, and clotted blood to the plastic tube walls [1]. The plastic PRT tubes used in the present study contained silica and surfactants coated on the surfaces of their interior walls to promote rapid clotting, which explains why the R and K times were similar to those for glass tubes [1]. The chemoPET tubes were made to have interior wall surfaces similar to those of glass to avoid having to coat their surfaces with surfactants, which have been shown to interfere with diagnostic tests [14]. The similar R and K times and MAs in both plastic and glass tubes demonstrated that chemical hydrophilization of the interior surfaces of plastic tube walls makes them a suitable alternative to glass tubes. It should be noted that RST, SST, and Vacuette tubes contain a separator gel to improve separation of serum from red blood cells and improve clot activation [38]. Therefore, in order to eliminate the effect of separator gel, they were not included in the TEG experiments.

Table 4
Performances of various tube types compared to chemoPET for FT_3 and FT_4 tests.

Tube type	FT_3		FT_4	
	Mean (SD) (pg/mL)	Bias[a] (%)	Mean (SD) (ng/dL)	Bias[a] (%)
Glass	2.77 ± 0.38	–	1.12 ± 0.14	–
ChemoPET	2.85 ± 0.46	3.01	1.15 ± 0.12	2.77
PRT	2.71 ± 0.39	−2.05	1.14 ± 0.13	1.87
RST™	2.72 ± 0.37	−1.69	1.15 ± 0.13	2.77
SST™	2.95 ± 0.41	**6.62**[b,c]	1.15 ± 0.14	2.77
Vacuette™	2.75 ± 0.42	−0.61	1.15 ± 0.11	2.77

All results are means ± standard deviation (SD).
[a] Biases are defined as deviations from values for the BD Glass tubes (control tubes).
[b] $P < 0.00833$ was considered statistically significant.
[c] Exceeded maximum desirable bias and is indicated in bold.

3.6. Specimen integrity

The present study evaluated plastic BCTs from various tube manufacturers. None demonstrated any significant differences from glass tubes in terms of specimen integrity as indicated by icterus and lipemia serum indices. This result is consistent with the results of our previous work [14]. The magnitude of hemolysis, icterus, and lipemia from the various BCTs appeared comparable and unlikely to influence the determination of the free thyroid hormone concentrations that were evaluated in this study.

No red blood cell hang-up or red cell film was observed on the interior surfaces of any BCTs. In addition, analysis found no clot adhesions on the surfaces of the tubes' interior walls, no microclots, and no latent clotting in any type of BCT. These findings supported those of our previous study, which found that the interior wall surfaces of chemoPET tubes performed as well as those of glass and other commercially available BCTs in preventing red blood cell adherence to the surfaces of interior walls [1].

3.7. Tubes compared to glass with serum specimens for FT_3 and FT_4 concentrations

As Table 4 shows, when serum FT_3 concentrations collected from various types of tubes were compared to glass tubes, no statistically significant differences were observed for Vacuette, RST, PRT, or chemoPET tubes.

However, the serum FT_3 concentrations collected in SST tubes were statistically significant when compared to the concentrations collected in glass tubes ($p = 0.0026$; Table 4). Serum FT_4 concentrations collected in the various types of tubes did not differ significantly from concentrations collected in glass tubes ($p = 0.96$; Table 4). The biases among the tube types for FT_3 and FT_4 concentrations ranged from −2.05% to 6.62% and from 1.87% to 2.77%, respectively. The maximum desirable bias for FT_3 (4.80%) was exceeded only when SSTs were compared to glass tubes (6.62%), and this was determined to be clinically significant. No type of tube exceeded the maximum desirable bias for FT_4 concentrations (3.30%) [14]. The SST tubes used to collect serum have several components, including tube-wall materials, surfactants, separator gels, and clot activators, either in the tubes or in or applied to the rubber stoppers, which have the potential to interfere with immunoassays [1]. We speculate that the clinically significant difference between serum FT_3 concentrations collected in SSTs and in the other BCT types is due to the surfactant(s) present in the SSTs. It has been shown that silicone surfactants (e.g., Silwet L-720) in SST BCTs can cause desorption and/or denaturation of antibodies on the surfaces of the polystyrene beads used in Immulite total thyroid hormone assays [2]. It is conceivable that the same mechanism of interference occurs in the FT_3 assay on the same instrument platform. Furthermore, it is possible that the type and concentration of surfactant in the SST tube differ from those in the other types of tubes, which may explain why the free thyroid hormone concentrations in the Vacuette, RST, and PRT tubes did not differ either significantly or clinically from those in the glass tubes. Previous studies have shown BCT lot-to-lot differences in assay results [2]. In fact, based on the authors' experiences, uneven spraying of tube additives on the surfaces of tube interior walls can be observed in many BCTs from various tube manufacturers, thus supporting that BCT additives and lot-to-lot differences in BCTs can have a significant effect on test results [2]. The chemoPET tubes contain no problematic surfactants, and this may explain the similarity between the free thyroid hormone results in chemoPET tubes and glass tubes [14]. Finally, unlike the FT_3 concentrations in the SST tubes, the FT_4 concentrations in that type of tube did not differ significantly or clinically when compared to the concentrations in glass tubes. The differences in BCT surfactant concentrations that are found in various immunoassays may explain why the FT_4 concentrations in the SSTs did not differ significantly or clinically from the concentrations in glass tubes. The thresholds at which surfactant interference becomes statistically and clinically significant may vary among immunoassays. Further studies are warranted to determine surfactant levels that cause significant interference in thyroid hormone assays.

The present study had some limitations. First, it examined only FT_3 and FT_4 concentrations in serum specimens that were collected in selected commercially available BCTs. There are many other immunology and chemistry analytes that are evaluated in a typical clinical-chemistry laboratory, but this study did not examine them. As such, the effects of types of tubes, including chemoPET tubes, on other serum analytes are unknown. Future work should test chemoPET tubes and other commercially available BCTs to identify the effects they may have on various clinical assays and a wide array of platforms. Second, the present study compared chemoPET tubes to five other types of serum tubes that are commonly used by clinical laboratories in North America. The study did not examine other commercially available serum tube types made by other manufacturers of blood collection tubes, including Sarstedt™ (Numbrecht, Germany) and Terumo™ (Leuven, Belgium). Future studies that compare other brands of serum BCTs to both chemoPET and glass tubes are warranted. Third, this study used only blood specimens collected from apparently healthy volunteers. Future studies that look at hospitalized patients who have significantly altered biochemistry values (abnormally low and high analyte concentrations) would be desirable to ascertain the performance of chemoPET tubes and other types of tubes in these diverse patient populations.

4. Conclusions

To understand the surface chemistry, topography, and surface dynamics of modified PET, surface modification of PET films was

performed by base-catalyzed transesterification with EG. The XPS results indicated an increased oxygen concentration and C—O/C=O ratio at the surface of modified samples. The ToF-SIMS results showed that modification increased the composition of fragments that had EG end groups. These results confirmed the success of grafting EG molecules to PET molecules on the surface. The effect of surface modification on surface energy was evaluated, and it was found that modification increased both surface tension and surface polarity, which indicated a shift to a very hydrophilic surface. The AFM images showed that the modification reaction significantly changed the surface topography, making it a very smooth surface that had nanometer-scaled, needle-like asperities. Estimation of Hansen solubility parameters based on PET and modified PET repeat units indicated that these asperities could be attributed to the molecular segregation of the modified PET molecules at the surface. The stability of surface modification was evaluated by tracking surface energy over 280 days, and a decrease in surface energy followed by a plateau after 190 days was observed. The XPS analysis showed a decreased C—O/C=O ratio after this period, which indicates a change in the surface chemistry toward a less-hydrophilic surface. The AFM results of the aged sample indicated that aging eliminated the small nanometer-scaled, needle-like features and increased the samples' roughness. All these results confirmed rearrangement of the modified surface toward lower energy and a very thermodynamically stable surface. The TEG results provided data on clot initiation, clot development, and clot strength, which were useful in evaluating and comparing the chemoPET tubes with other commercially available blood collection tubes. The plastic chemoPET tubes showed coagulation performance similar to that of both glass tubes and commercially available plastic tubes that have substances applied to the surfaces of their interior walls to accelerate coagulation.

This study found that the interior surfaces of the newly developed chemically modified plastic tubes achieved results comparable to those of commercially available plastic serum BCTs when used with free thyroid hormones on the Immulite 1000 platform. We recommend use of these new chemoPET tubes, which contain no proprietary surfactants, rather than commercially available plastic BCTs that contain problematic surfactants, thereby minimizing the unpredictable interference of surfactants on some clinical assays.

Acknowledgements

The authors would like to thank Mr. Simon Ng for performing the thromboelastography on the different tube types.

References

[1] R.A.R. Bowen, G.L. Hortin, G. Csako, O.H. Otañez, A.T. Remaley, Impact of blood collection devices on clinical chemistry assays, Clin. Biochem. 43 (2010) 4–25.
[2] R.A.R. Bowen, Y. Chan, M.E. Ruddel, G.L. Hortin, G. Csako, S.J. Demosky, A.T. Remaley, Immunoassay interference by a commonly used blood collection tube additive, the organosilicone surfactant Silwet L-720, Clin. Chem. 51 (2005) 1874–1882.
[3] W. Chen, T.J. McCarthy, Chemical surface modification of poly(ethylene terephthalate), Macromolecules 31 (1998) 3648–3655.
[4] A.Y. Fadeev, T.J. McCarthy, Surface modification of poly(ethylene terephthalate) to prepare surfaces with silica-like reactivity, Langmuir 14 (1998) 5586–5593.
[5] N. Inagaki, K. Narushim, N. Tuchida, K. Miyazaki, Surface characterization of plasma-modified poly(ethylene terephthalate) film surfaces, J. Polym. Sci., Part B: Polym. Phys. 42 (2004) 3727–3740.
[6] K.G. Kostov, T.M.C. Nishime, A.H.R. Castro, A. Toth, L.R.O. Hein, Surface modification of polymeric materials by cold atmospheric plasma jet, Appl. Surf. Sci. 314 (2014) 367–375.
[7] E. Gonzalez, M.D. Barankin, P.C. Guschl, R.F. Hicks, Remote atmospheric-pressure plasma activation of the surfaces of polyethylene terephthalate and polyethylene naphthalate, Langmuir 24 (2008) 12636–12643.
[8] X. Ping, M. Wang, G. Xuewu, Surface modification of poly(ethylene terephthalate) (PET) film by gamma-ray induced grafting of poly(acrylic acid) and its application in antibacterial hybrid film, Radiat. Phys. Chem. 80 (2011) 567–572.
[9] F. Rezaei, M.D. Dickey, M. Bourham, P.J. Hauser, Surface modification of PET film via a large area atmospheric pressure plasma: an optical analysis of the plasma and surface characterization of the polymer film, Surf. Coat. Technol. 309 (2017) 371–381.
[10] Y. Ikada, Surface modification of polymers for medical applications, Biomaterials 15 (1994) 725–736.
[11] Y.L. Hsieh, D.A. Timm, M. Wu, Solvent- and glow-discharge-induced surface wetting and morphological changes of poly(ethylene terephthalate) (PET), J. Appl. Polym. Sci. 38 (1989) 1719–1737.
[12] B. Gupta, J. Hilborn, C. Hollenstein, C. Plummer, R. Houriet, N. Xanthopoulos, Surface modification of polyester films by RF plasma, J. Appl. Polym. Sci. 78 (2000) 1083–1091.
[13] A. Vesel, M. Mozetic, A. Zalar, XPS study of oxygen plasma activated PET, Vacuum 82 (2007) 248–251.
[14] S. Kim, R.A.R. Bowen, R.N. Zare, Transforming plastic surfaces with electrophilic backbones from hydrophobic to hydrophilic, ACS Appl. Mater. Interfaces 7 (2015) 1925–1931.
[15] S. Scarpelini, S.G. Rhind, B. Nascimento, H. Tien, P.N. Shek, H.T. Peng, H. Huang, R. Pinto, V. Speers, M. Reis, S.B. Rizoli, Normal range values for thromboelastography in healthy adult volunteers, Braz. J. Med. Biol. Res. 42 (2009) 1210–1217.
[16] H.T. Peng, Thromboelastographic study of biomaterials, J. Biomed. Mater. Res. B Appl. Biomater. 94B (2010) 469–485.
[17] G. Dimeski, J. Johnston, P. Masci Paul, K.-N. Zhao, N. Brown, Evaluation of the Greiner bio-one serum separator BCA fast clot tube, Clin. Chem. Lab. Med. (CCLM) (2017) 1135.
[18] D.K. Owens, R.C. Wendt, Estimation of the surface free energy of polymers, J. Appl. Polym. Sci. 13 (1969) 1741–1747.
[19] R.J. Good, Contact angle, wetting, and adhesion: a critical review, J. Adhes. Sci. Technol. 6 (1992) 1269–1302.
[20] F.R. Lang, Y. Pitton, H.J. Mathieu, D. Landolt, E.M. Moser, Surface analysis of polyethyleneterephthalate by ESCA and TOF-SIMS, Anal. Bioanal. Chem. 358 (1997) 251–254.
[21] M. Wegelin, S. Canonica, C. Alder, D. Marazuela, M.F. Suter, T.D. Bucheli, O. Haefliger, R. Zenobi, K. McGuigan, M. Kelly, Does sunlight change the material and content of polyethylene terephthalate (PET) bottles, J. Water Supply: Res. Technol.-AQUA 50 (2001) 125–135.
[22] L. Li, K.M. Ng, C.M. Chan, J.Y. Feng, X.M. Zeng, L.T. Weng, Surface studies of the rearrangement of end groups of a polymer by ToF–SIMS and AFM, Macromolecules 33 (2000) 5588–5592.
[23] S. Wu, Interfacial and surface tensions of polymers, J. Macromol. Sci., Part C 10 (1974) 1–73.
[24] L. Van Krevelen, K. Nijenhuis, Properties of Polymers, Elsevier, Slovenia, 2009.
[25] L. Bicerano, Prediction of Polymer Properties, Marcel Dekker, New York, 2002.
[26] A. Agrawal, A.D. Saran, S.S. Rath, A. Khanna, Constrained nonlinear optimization for solubility parameters of poly(lactic acid) and poly(glycolic acid)—validation and comparison, Polymer 45 (2004) 8603–8612.
[27] H. Assender, V. Bliznyuk, K. Porfyrakis, How surface topography relates to materials' properties, Science 297 (2002) 973–976.
[28] B. Gupta, C. Plummer, I. Bisson, P. Frey, J. Hilborn, Plasma-induced graft polymerization of acrylic acid onto poly(ethylene terephthalate) films: characterization and human smooth muscle cell growth on grafted films, Biomaterials 23 (2002) 863–871.
[29] Z.Y. Zhang, I.W. Boyd, H. Esrom, Surface modification of polyethylene terephthalate with excimer UV radiation, Surf. Interface Anal. 24 (1996) 718–722.
[30] J. Deng, L. Wang, L. Liu, W. Yang, Developments and new applications of UV-induced surface graft polymerizations, Prog. Polym. Sci. 34 (2009) 156–193.
[31] S.L. Gao, R. Habler, E. Mader, T. Bahners, K. Opwis, E. Schollmeyer, Photochemical surface modification of PET by excimer UV lamp irradiation, Appl. Phys. B 81 (2005) 681–690.
[32] Z. Zhu, M.J. Kelley, Poly(ethylene terephthalate) surface modification by deep UV (172nm) irradiation, Appl. Surf. Sci. 236 (2004) 416–425.
[33] P.S. Curti, M.R.D. Moura, W. Veiga, E. Radovanovic, A.F. Rubira, E.C. Muniz, Characterization of PNIPAAm photografted on PET and PS surfaces, Appl. Surf. Sci. 245 (2005) 223–233.
[34] E. Uchida, Y. Ikada, Topography of polymer chains grafted on a polymer surface underwater, Macromolecules 30 (1997) 5464–5469.
[35] H.J. Vandenburg, A.A. Clifford, K.D. Bartle, R.E. Carlson, J. Carroll, I.D. Newton, A simple solvent selection method for accelerated solvent extraction of additives from polymers, Analyst 124 (1999) 1707–1710.
[36] D.S. Pearson, L.J. Fetters, W.W. Graessley, G. Ver Strate, E. von Meerwall, Viscosity and self-diffusion coefficient of hydrogenated polybutadiene, Macromolecules 27 (1994) 711–719.
[37] S. Yavaş, S. Ayaz, S. Köse, F. Ulus, A. Ulus, Influence of blood collection systems on coagulation tests, Turk. J. Haematol. 29 (2012) 367–375.
[38] W.R. Fiehler, Blood serum separator tube, 1990.